

## **Role of surface profiles in surface plasmon-polariton-mediated emission of light through a thin metal film**

ARMANDO GIANNATTASIO\*, STEPHEN WEDGE  
and WILLIAM L. BARNES

School of Physics, University of Exeter, Stocker Road,  
Exeter EX4 4QL, UK

*(Received 15 September 2005)*

We show that the emission of light mediated by surface plasmon-polaritons through a thin metal film depends sensitively on the profile of the grating structure used to couple the surface plasmon-polariton modes to light. In particular, we show that when the emission of light takes place through a metal film, a non-conformal geometry for the two surfaces of the metal film is to be preferred. Our results may be important in the design of devices such as organic light-emitting diodes.

### **1. Introduction**

The field of organic light-emitting diodes (OLEDs) continues to be pursued very actively and is rapidly becoming of significant commercial interest. Recently, several research laboratories have begun to explore top-emitting OLEDs where light is emitted through an optically thin metallic cathode [1, 2], rather than substrate-emitting structures where emission typically takes place through an indium tin oxide (ITO) anode into the glass substrate [3, 4]. In both top- and substrate-emitting OLEDs, the role of surface plasmon-polaritons (SPPs) in the emission process is also of topical concern [5, 6].

Light is produced in OLEDs when excitons formed by the injection of opposite charges decay radiatively. However, light is not the only possible result of such decay, excitons may also decay by coupling to SPPs [7]. SPPs are guided modes that propagate at metal/dielectric interfaces and comprise an oscillation in the surface charge density within the metal together with an associated oscillating electromagnetic field. The surface nature of the mode is reflected in the fact that, for a single interface structure, the field decays exponentially with distance from the interface that supports the mode. The metallic layers frequently found in OLED devices for charge injection, for example metallic cathodes, often support SPP modes. SPPs are

---

\*Corresponding author. Email: a.giannattasio@ex.ac.uk

non-radiative on planar surfaces [8], they have too much momentum to be able to couple to free space photons, hence energy coupled to SPP modes cannot emerge from the device and energy coupled from excitons to SPPs is, in general, lost as heat.

The decay of excitons within an organic emissive material to SPP modes supported by a metallic cathode has been shown to account for up to 40% of the power that might otherwise be radiated [6]; SPPs thus represent a potentially very serious limitation on device performance. The extent of this problem depends strongly on the orientation of the dipole moment associated with the excitons. This is because fields normal to the surface are required if one is to induce charges at the surface, as is required for the excitation of SPP modes. In polymer devices where the dipole moments lie in the plane of the device and thus couple only weakly to SPP modes, the problem is less severe [6]. In dendrimer and small molecule based devices the problem is much more significant, accounting for up to 40% of the power. For this reason, several recent studies have looked at the possibility of converting such SPP modes back to light by using either wavelength scale gratings [5, 9] or inherent surface roughness [10] with the aim of recovering some of this lost energy. Such schemes allow the momentum of a SPP to be matched to the momentum of photons in air, thus enabling SPP-mediated emission of light [11–14].

In a top-emitting device, where the metallic cathode is of the order of tens of nanometres thick, the organic emissive layer may couple to SPP modes associated with both the metal/organic and metal/air interfaces. Calculations have shown a large disparity between the strength of coupling between the emitter and these two SPP modes, with the power lost to metal/organic SPP being approximately 100 times greater than the power dissipated to the metal/air SPP [9, 11].

## 2. Experiment and discussion

As noted above, by corrugating the structure on the scale of the wavelength of light, power lost to SPP modes may be recovered, a process that can be more than 50% efficient [15, 16]. We studied two samples to investigate this. The first sample [9] consisted of a 60 nm thick emissive layer of tris(8-hydroxyquinoline)aluminium ( $\text{Alq}_3$ ) thermally evaporated onto a silica grating (pitch 338 nm, sinusoidal profile) fabricated over an area of approximately  $1 \text{ cm}^2$ . In turn, a 55 nm thick silver film was then evaporated on the  $\text{Alq}_3$  layer in order to obtain a silica/ $\text{Alq}_3$ /silver/air corrugated interface with a sinusoid-shaped profile. A more complete description of the fabrication of this sample can be found elsewhere [9], a schematic and SEM cross-section are shown in figure 1(a).

Since we were interested here only in the underlying physics of the coupling of the SPP modes to light, it was sufficient to measure the SPP-mediated photoluminescence (PL) emission from an emissive layer through a thin silver film. The sample was mounted on a rotation stage and the  $\text{Alq}_3$  layer was optically pumped through the silica substrate by a 410 nm laser. The intensity of the PL transmitted through the silver into the air was measured as a function of the emission angle in the plane normal to the sample surface and to the grating grooves (the classical mount). The PL spectrum was recorded using a spectrometer/CCD combination with a spectral

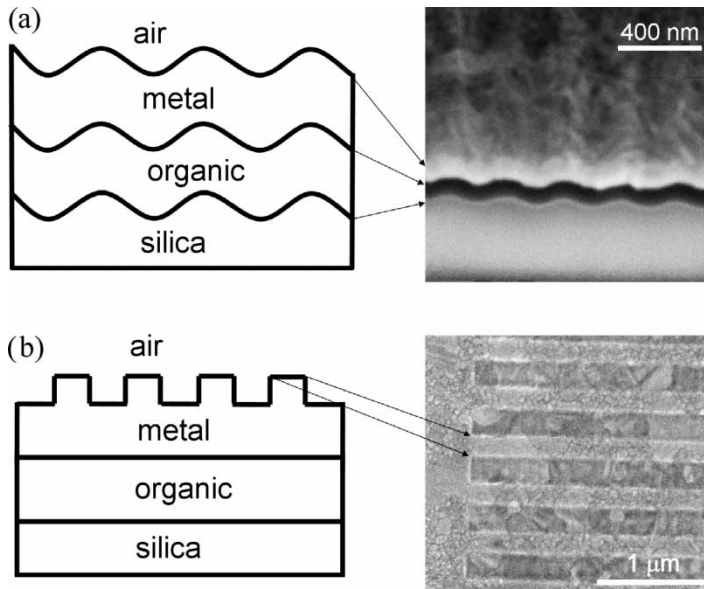


Figure 1. Schematic of the two structures investigated in this work. SEM pictures of the samples used in the experiment are also shown on the right-hand side of this figure. The upper panels (a) show the structure that has a metallic film with a grating profile on top and bottom surfaces. The lower panel (b) shows the structure for which only the top surface of the metal is textured. The SEM in (a) is a cross-section taken at an angle of  $52^\circ$ , whereas the SEM in (b) is a plan view.

resolution of 2 nm. A polarizer was placed just before the spectrometer entrance and set to pass TM polarized light only. The angular resolution during the collection of the data was limited to approximately  $1^\circ$  by the use of a narrow aperture. Using data acquired in this way we could plot the PL intensity as a function of frequency and in-plane wavevector (the component of the wavevector in the plane of the structure) (figure 2a); the contribution and dispersion of the metal/organic and metal/air SPP modes is clearly seen.

It is apparent from figure 2(a) that the disparity in the coupling strength between the emitter and the SPP modes associated with either side of a thin metal film is not seen in the SPP-mediated photoluminescence (PL) emission. Instead, both SPP modes exhibit a similar emission intensity, indeed if anything the emission associated with the metal/air interface is stronger—it is light associated with this mode that was seen by Köck *et al.* [17].

One might perhaps have thought that the much weaker than expected presence of emission from the SPP associated with the metal/organic interface might be due to the attenuation that light must undergo in crossing the metal film as it leaves the device. However, the cause of the relatively weak emission associated with the metal/organic SPP (when compared with the strength with which the emitter couples to the two SPP modes) is much more subtle and, as we show below, can be overcome through careful control of the shape of the periodic corrugation.

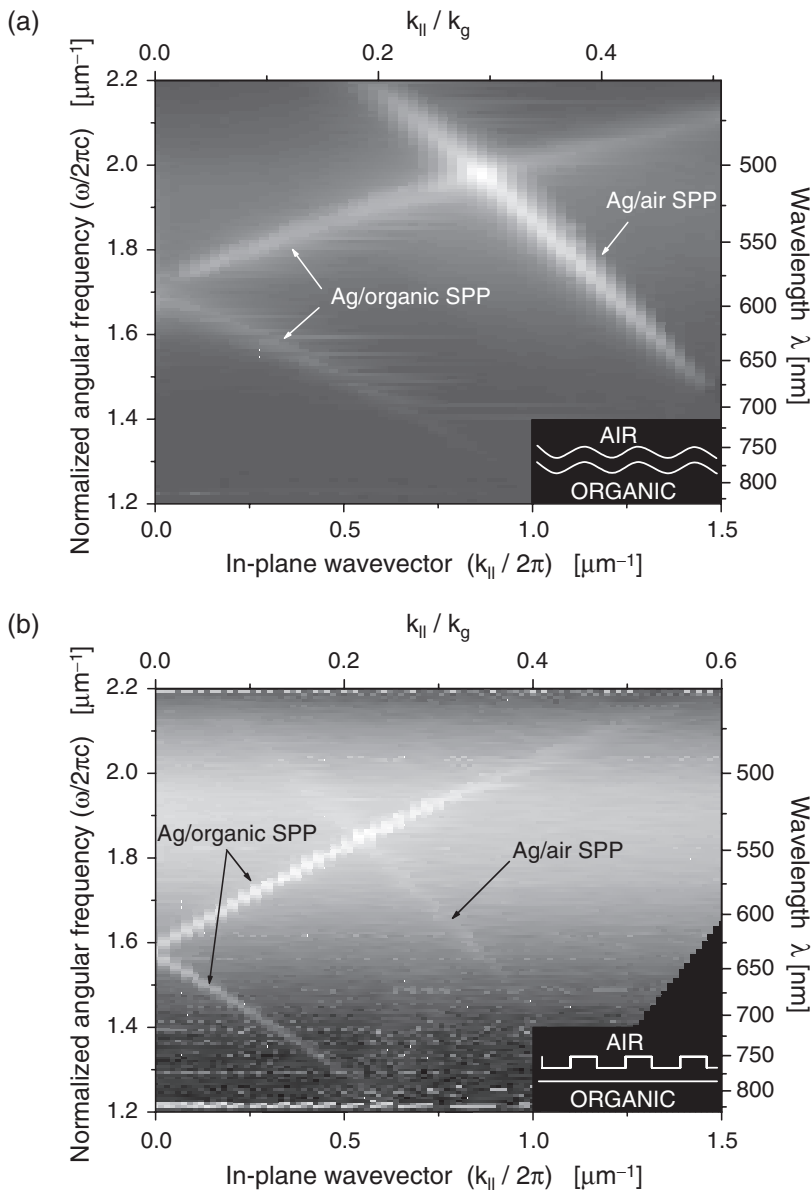


Figure 2. Dispersion maps constructed from SPP-mediated photoluminescence data. The upper panel (a) shows data for the conformal structure presented in figure 1(a) (metal has same grating profile on top and bottom surfaces, period of grating is 338 nm); the lower panel (b) contains data from the sample shown in figure 1(b) (metal is only textured on top surface, period of grating is 400 nm). The lower resolution of data in (a) compared with that in (b) is due to the much smaller area of the grating used in the second sample, hence the weak SPP-coupled photoluminescence intensity compared with the background light emission from the dye layer. The background emission present in (b) is the direct emission from Alq<sub>3</sub>.

The reason that emission mediated by the SPP associated with the metal/organic interface is weak arises from destructive interference between two possible pathways by which emission from this mode may occur [18, 19]; the argument is as follows. Consider a structure such as that shown schematically in figure 1(a), where a corrugation has been introduced into a top-emitting OLED structure with the aim of recovering power lost to SPP modes. We are interested in the emission of light mediated by the SPP mode associated with the metal/organic interface. This mode can be coupled by the grating to light via two different routes [11]. The first route involves the SPP being scattered by the grating at the metal/organic interface; light generated in this process is attenuated across the metal film and reaches the air without experiencing any further scattering event. The second route is when the SPP is scattered by the grating present at the metal/air interface. This is possible because the field distribution of the SPP associated with the metal/organic interface extends through the metal film to the metal/air interface; in this case there is also attenuation, this time associated with the field of the SPP that spans the metal. Both of these mechanisms involve attenuation across the metal film—they therefore have similar amplitudes, the intensity of the resulting emission thus depends on the relative phase of these two routes.

To gain insight into the phase of the scattered light it is instructive to look at the expression for the amplitude coefficient,  $t_1$ , of the first diffracted order for light scattered by a corrugated interface between media of relative permittivity  $\varepsilon_1$  and  $\varepsilon_2$  [18, 19],

$$t_1 = \frac{i(\varepsilon_2 - \varepsilon_1)k_0^3 h \gamma_r \sqrt{\varepsilon_2}}{2(\gamma_t + \gamma_r)(k_g^2 + \gamma_r \gamma_t)} \left( \frac{2\sqrt{\varepsilon_1}}{\sqrt{\varepsilon_1} + \sqrt{\varepsilon_2}} \right),$$

where  $k_0$  is the free space wavevector, and  $k_g$  is the wavevector associated with the corrugation ( $k_g = 2\pi/\lambda_g$ , where  $\lambda_g$  is the pitch of the corrugation). The coefficients  $\gamma_r$  and  $\gamma_t$  are the wavevector components along the  $z$  axis of the reflected and transmitted electromagnetic field, respectively [19]. The key point of concern in the present context is the factor  $(\varepsilon_2 - \varepsilon_1)$  in the numerator. Since many metals have a largely negative real relative permittivity in the spectral region of interest, whilst the bounding dielectrics have positive real relative permittivities, this term is of opposite sign for scattering out from the metal/air interface when compared to scattering out from the organic/metal interface. Thus, for the structure shown in figure 1(a), light produced as a result of scattering from the lower corrugation is out of phase with light produced by scattering from the upper corrugation. The resulting destructive interference between the two [18, 20] accounts for the much weaker than expected contribution to the emitted light of the metal/organic SPP from structures such as those shown in figure 1(a). As a consequence, the efficiency of an OLED based on such a design would be reduced if this symmetry were used to fabricate the periodic structure.

To overcome this reduction in output due to destructive interference, one needs either to shift the phase of the two grating surfaces, or to eliminate one of the grating surfaces. To demonstrate that this can be done, we fabricated a structure with a different geometry. A flat silica substrate was spin-coated at a rate of 4000 rpm with

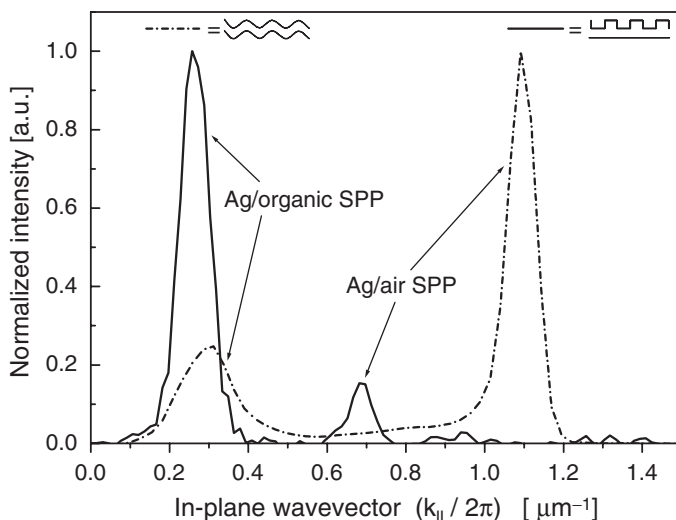


Figure 3. Normalized PL intensity measured for two samples having different interface profiles (shown in the inset). A significant increase in PL emission due to the excitation of SPPs at the Ag/organic interface is observed when the profiles of the two interfaces are not symmetric (solid line). Data represented by the solid line were taken at a wavelength of 580 nm, whereas data corresponding to the dashed-dot line were taken at 550 nm (see also figure 2).

a solution of polymethylmethacrylate (PMMA) and Alq<sub>3</sub> (3% by weight) in chloroform. The thickness of the PMMA/Alq<sub>3</sub> organic film deposited with this procedure was approximately 160 nm. Subsequently, a silver film of thickness  $(50 \pm 1)$  nm was thermally evaporated on top of the organic layer at a pressure of  $\sim 3 \times 10^{-7}$  mbar. A periodic corrugation was then introduced at the metal/air interface using a Focused Ion-Beam milling system (FEI Nova 600). The corrugation consisted of a grating with square profile having a pitch of 400 nm and a depth of 15 nm; the grating area covered a total of  $95 \mu\text{m} \times 190 \mu\text{m}$ ; a schematic and SEM micrograph are shown in figure 1(b).

An experimentally derived dispersion map for this second sample is shown in figure 2(b), again formed using the PL intensity as a function of frequency and in-plane wavevector. As with the first sample, the SPP mode associated with the metal/organic interface and the SPP mode associated with the metal/air interface are both seen. Although the form of the data shown in figure 2(b) is very similar to that shown in figure 2(a), there is a striking difference in the relative intensity of light associated with the two SPP modes. The intensity of emission associated with the metal/organic SPP is now seen to be greater than that observed for the metal/air SPP. This is even more evident when single spectra for the two samples are compared, as shown in figure 3. In this figure, the normalized PL intensity is plotted as a function of the in-plane wavevector for a given value of angular frequency ( $1.82 \mu\text{m}^{-1}$  for the symmetric and  $1.72 \mu\text{m}^{-1}$  for the asymmetric structure). The graph in figure 3 shows that, in the presence of an asymmetric profile of the

two interfaces (solid line), there is a very significant increase in PL intensity due to radiative SPPs excited at the Ag/organic boundary compared with the intensity associated with the SPPs excited at the Ag/air boundary. These data are consistent with the ideas outlined above, namely that, by removing one of the pathways for emission of the metal/organic SPP, the possibility of destructive interference is removed, resulting in more emission mediated by the SPP associated with the Ag/organic interface being observed.

### 3. Conclusions

Our results suggest that the efficiency of organic light-emitting devices might be increased simply by using a non-conformal geometry for the different metallic interfaces. One might hope that greater improvements in the extraction efficiency of light mediated by the metal/organic interface would be possible if, rather than removing one corrugation, the two corrugations were instead shifted in phase by  $\pi$ . We note that metallic hole arrays might serve this purpose [21], and further note that, as for the second structure we explored here, it is not necessary that the film be perforated, a suitably modulated film would suffice [22, 23]. The work reported here extends the number of structures that have been demonstrated to allow at least some of the power lost to this SPP mode to be recovered. Considerable further investigation is needed to identify the best approaches and to explore their practical applicability.

### Acknowledgments

We would like to thank I. R. Hooper for useful discussions. The support of this work by the EC funded project 'Surface Plasmon Photonics' NMP4-CT-2003-505699 is gratefully acknowledged.

### References

- [1] V. Bulovic, G. Gu, P.E. Burrows, *et al.*, *Nature* **380** 29 (1996).
- [2] M.-H. Lu, M.S. Weaver, T.X. Zhou, *et al.*, *Appl. Phys. Lett.* **81** 3921 (2002).
- [3] C.W. Tang and S.A. VanSlyke, *Appl. Phys. Lett.* **51** 913 (1987).
- [4] J.H. Burroughes, D.D.C. Bradley, A.R. Brown, *et al.*, *Nature* **347** 539 (1990).
- [5] P.A. Hobson, S. Wedge, J.A.E. Wasey, *et al.*, *Adv. Mater.* **14** 1393 (2002).
- [6] J.M. Ziebarth and M.D. McGehee, *J. Appl. Phys.* **97** 064502 (2005).
- [7] W.H. Weber and C.F. Eagan, *Optics Lett.* **4** 236 (1979).
- [8] H. Raether, *Surface Plasmons* (Springer, Berlin, 1988).
- [9] S. Wedge and W.L. Barnes, *Opt. Express* **12** 3673 (2004).
- [10] R. Windisch, S. Schoberth, S. Meinschmidt, *et al.*, *J. Optics A* **1** 512 (1999).
- [11] S. Wedge, I.R. Hooper, I. Sage, *et al.*, *Phys. Rev. B* **69** 245418 (2004).
- [12] W.L. Barnes, *Nat. Mater.* **3** 588 (2004).
- [13] K. Okamoto, I. Niki, A. Shvartser, *et al.*, *Nat. Mater.* **3** 601 (2004).
- [14] D.K. Gifford and D.G. Hall, *Appl. Phys. Lett.* **80** 3679 (2002).

- [15] J. Moreland, A. Adams and P.K. Hansma, *Phys. Rev. B* **25** 2297 (1982).
- [16] P.T. Worthing and W.L. Barnes, *J. Mod. Optics* **49** 1453 (2002).
- [17] A. Köck, E. Gornik, M. Hauser, *et al.*, *Appl. Phys. Lett.* **57** 2327 (1990).
- [18] I.R. Hooper and J.R. Sambles, *Phys. Rev. B* **67** 235404 (2003).
- [19] J.-J. Greffet and Z. Maasarani, *J. Opt. Soc. Am. A* **7** 1483 (1990).
- [20] I.R. Hooper and J.R. Sambles, *Phys. Rev. B* **70** 045421 (2004).
- [21] T.W. Ebbesen, H.J. Lezec, H.F. Ghaemi, *et al.*, *Nature* **391** 667 (1998).
- [22] I. Avrutsky, *Phys. Rev. B* **70** 155416 (2004).
- [23] N. Bonod, S. Enoch, L.F. Li, *et al.*, *Opt. Express* **11** 482 (2003).